

# Formation of the Ionic Gold(III) Complex [Au<sub>3</sub>{S<sub>2</sub>CN(CH<sub>2</sub>)<sub>4</sub>O}<sub>6</sub>][Au<sub>2</sub>Cl<sub>8</sub>][AuCl<sub>4</sub>] in Chemisorption Systems [M{S<sub>2</sub>CN(CH<sub>2</sub>)<sub>4</sub>O}<sub>2</sub>]<sub>n</sub>–[AuCl<sub>4</sub>]<sup>–</sup>/2 M HCl (M = Cd, Zn): Supramolecular Structure and Thermal Behavior

T. A. Rodina<sup>a, b</sup>, O. V. Loseva<sup>a</sup>, A. V. Ivanov<sup>a, \*</sup>, A. V. Gerasimenko<sup>c</sup>, V. I. Sergienko<sup>c</sup>,  
A. S. Zaeva<sup>a</sup>, and E. V. Korneeva<sup>a</sup>

<sup>a</sup> Institute of Geology and Nature Management, Far East Branch, Russian Academy of Sciences,  
Relochnyi per. 1, Blagoveshchensk, 675000 Russia

<sup>b</sup> Amur State University, Blagoveshchensk, 675027 Russia

<sup>c</sup> Institute of Chemistry, Far East Branch, Russian Academy of Sciences,  
pr. Stoletiya Vladivostoka 159, Vladivostok, 690022 Russia

\*e-mail: alexander.v.ivanov@chemist.com

Received March 4, 2013

**Abstract**—The interaction of freshly precipitated cadmium and zinc morpholinedithiocarbamates with solutions of AuCl<sub>3</sub> in 2 M HCl is studied. In both cases, the heterogeneous reactions of gold(III) binding from solutions lead to the formation of the ionic gold(III) complex [Au<sub>3</sub>{S<sub>2</sub>CN(CH<sub>2</sub>)<sub>4</sub>O}<sub>6</sub>][Au<sub>2</sub>Cl<sub>8</sub>][AuCl<sub>4</sub>] (**I**), whose molecular and supramolecular structures are determined by X-ray diffraction analysis. Compound **I** includes centrosymmetric and noncentrosymmetric cations [Au{S<sub>2</sub>CN(CH<sub>2</sub>)<sub>4</sub>O}<sub>2</sub>]<sup>+</sup> in a ratio of 1 : 2. According to the manifested structural differences, the complex cations are related as conformers (cations A are Au(1) and cations B are Au(2)). At the supramolecular level, the isomeric cations form linear trinuclear structural fragments [Au<sub>3</sub>{S<sub>2</sub>CN(CH<sub>2</sub>)<sub>4</sub>O}<sub>6</sub>]<sup>3+</sup> [A···B···A] due to secondary bonds Au···S of 3.6364 Å. The anionic part of compound **I** is presented by [AuCl<sub>4</sub>]<sup>–</sup> and centrosymmetric binuclear [Au<sub>2</sub>Cl<sub>8</sub>]<sup>2–</sup>, whose formation involved secondary bonds Au···Cl of 3.486 and 3.985 Å. The ultimate chemisorption capacity of cadmium and zinc morpholinedithiocarbamates calculated from the binding of gold(III) is 901.7 and 1010.4 mg of Au<sup>3+</sup> per 1 g of the sorbent, respectively (i.e., each miononuclear fragment of the chemisorption complexes [M{S<sub>2</sub>CN(CH<sub>2</sub>)<sub>4</sub>O}<sub>2</sub>]<sub>n</sub> participates in binding of two gold atoms). To establish the conditions for the isolation of bound gold, the thermal properties of compound **I** are studied by simultaneous thermal analysis. The thermal destruction process includes the thermolysis of the dithiocarbamate part of the complex and anions [AuCl<sub>4</sub>]<sup>–</sup> and [Au<sub>2</sub>Cl<sub>8</sub>]<sup>2–</sup> with the reduction of gold to the metal, being the only final product of the thermal transformations of compound **I**.

**DOI:** 10.1134/S1070328413100072

## INTRODUCTION

Dithiocarbamate complexes are promising precursors in one-stage processes of the preparation of film and nanosized cadmium [1–6] and zinc [6–10] sulfides. Another practically important property of the dithiocarbamate complexes is their capability of binding gold from solutions to form diverse polynuclear and heteropolynuclear compounds [11–15]. We have previously shown [16] that the interaction of cadmium morpholinedithiocarbamate with moderately concentrated solutions of gold(III) chloride affords the hydrated form of a gold(III)–cadmium heteropolynuclear complex ([Au{S<sub>2</sub>CN(CH<sub>2</sub>)<sub>4</sub>O}<sub>2</sub>]<sub>2</sub>[CdCl<sub>4</sub>] · H<sub>2</sub>O)<sub>n</sub> including four structurally nonequivalent complex cations [Au{S<sub>2</sub>CN(CH<sub>2</sub>)<sub>4</sub>O}<sub>2</sub>]<sup>+</sup> (A, B, C, D) in a ratio of 1 : 1 : 1 : 1. The structural organization of the complex at the supramolecular level seemed unusual,

because pairs of the discussed cations formed two independent polymer chains (–A–C–)<sub>n</sub> and (–B–D–)<sub>n</sub> due to nonequivalent secondary bonds Au···S. However, tetrachlorocadmite ions can be replaced by tetrachloroaurate ones in the region of more concentrated solutions of AuCl<sub>3</sub>, which assumes a dramatic rearrangement of the initial structural type of the gold(III)–cadmium complex [16]. The gold(III) and gold(I) complexes with dithio ligands (dithiocarbamates and dithiophosphates) are of practical interest, since they manifest properties of highly efficient anticancer drugs [17], sensors of chemical volatiles [18], and luminophores [19–21].

In this work, the interaction of freshly precipitated cadmium (sorbent **Ia**) and zinc (**Ib**) morpholinedithiocarbamates (Mfdtc) with solutions of AuCl<sub>3</sub> in 2 M HCl was studied and their sorption capacity was established. The heterogeneous reactions that proceed via the chemi-

sorption mechanism were shown to include the partial ion exchange and are accompanied by the formation of the polynuclear gold(III) complex  $[\text{Au}_3\{\text{S}_2\text{CN}(\text{CH}_2)_4\text{O}\}_6][\text{Au}_2\text{Cl}_8][\text{AuCl}_4]$  (**I**). The molecular and crystal structures of preparatively isolated compound **I** were determined by X-ray diffraction analysis. The thermal properties of compound **I** were studied by simultaneous thermal analysis (STA).

## EXPERIMENTAL

Sodium morpholinedithiocarbamate was prepared by the reaction of carbon bisulfide (Merck) and morpholine (Aldrich) in an alkaline medium [22]. The starting cadmium (**Ia**) [23, 24] and zinc (**Ib**) [25] complexes were synthesized by the precipitation of  $\text{Cd}^{2+}$  and  $\text{Zn}^{2+}$  ions from the aqueous medium with  $\text{NaMfdtc}$  taken in a stoichiometric ratio. The initial salt and complexes **Ia** and **Ib** were characterized by  $^{13}\text{C}$  MAS NMR spectroscopy ( $\delta$ , ppm):

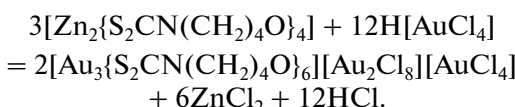
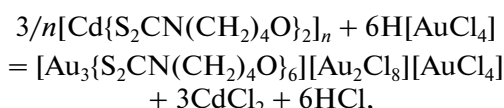
$\text{Na}\{\text{S}_2\text{CN}(\text{CH}_2)_4\text{O}\} \cdot 2\text{H}_2\text{O}$  (1 : 2 : 2) : 204.8 ( $-\text{S}_2\text{CN}=$ ); 67.6, 67.2 ( $-\text{OCH}_2-$ ); 54.6, 53.9, 53.5 ( $=\text{NCH}_2-$ ).

$[\text{Cd}\{\text{S}_2\text{CN}(\text{CH}_2)_4\text{O}\}_2]_n$ : 204.2 (52)\* ( $-\text{S}_2\text{CN}=$ ); 67.0, 66.4, 65.8 (1 : 1 : 2,  $-\text{OCH}_2-$ ); 54.6, 54.2, 53.6, 53.4 ( $\sim 1 : 4 : 3 : 2$ ,  $=\text{NCH}_2-$ ).

$[\text{Zn}_2\{\text{S}_2\text{CN}(\text{CH}_2)_4\text{O}\}_4]$ : 200.4 (61)\*, 199.7 (60)\* (1 : 1,  $-\text{S}_2\text{CN}=$ ); 67.4, 67.1 (1 : 3,  $-\text{OCH}_2-$ ); 54.3, 53.6, 52.8, 50.8 (1 : 1 : 1 : 1,  $=\text{NCH}_2-$ ).

(\* Asymmetric  $^{13}\text{C}$ – $^{14}\text{N}$  doublets [26, 27], in Hz.)

**Synthesis of hexakis(morpholinedithiocarbamato-*S,S*)trigold(III) tetrachloroaurate(III)-octachlorodaurate(III) (**I**)** was carried out by the heterogeneous reactions of freshly prepared cadmium and zinc morpholinedithiocarbamates and solutions of  $\text{AuCl}_3$  in 2 M HCl proceeding via the chemisorption mechanism (including the partial ion exchange)



A solution of  $\text{AuCl}_3$  (in 2 M HCl) containing 89.4 or 100.5 mg of gold was poured to 100 mg of cadmium or zinc morpholinedithiocarbamate, respectively, and the mixture was stirred for 2.5 h. Obtained yellow-orange precipitates were filtered off, dried on the filter, and dissolved in acetone with moderate heating. Transparent yellow prismatic crystals of complex **I** suitable for diffraction experiment were obtained from acetone.

$^{13}\text{C}$  MAS NMR data: 198.4, 195.0, 190.6 ppm (1 : 1,  $-\text{S}_2\text{CN}=$ ); 67.6, 66.7, 66.0 (1 : 2 : 3,  $-\text{OCH}-$ ); 52.3, 51.4, 49.7 (1 : 1 : 4,  $=\text{NCH}_2-$ ).

**Gold(III) sorption** was carried out in the static mode. A solution of  $\text{AuCl}_3$  (10 mL) containing 89.40 or 100.47 mg of gold(III), which is close to the calculated values of the ultimate chemisorption capacity, was poured to portions (100 mg) of freshly precipitated sorbents **Ia** or **Ib**, respectively. The mixture was magnetically stirred for 1–90 min at ambient temperature. Portions (0.1 mL) of the solution were taken at certain intervals to determine the residual concentration of gold. The degree of extraction ( $S$ , %) was calculated using the formula

$$S = [(c - c_0)/c] \times 100,$$

where  $c$  and  $c_0$  are the initial and residual gold contents in the solution, respectively. The concentration of absorbed gold(III) was determined from this difference. The gold content in solutions was determined on an atomic absorption spectrometer (1 class, Hitachi, model 180-50).

$^{13}\text{C}$  MAS NMR spectra were recorded on a CMX-360 spectrometer (Agilent/Varian/Chemagnetics InfinityPlus) with a working frequency of 90.52 MHz, a superconducting magnet ( $B_0 = 8.46$  T), and Fourier transform. Proton cross polarization was used for  $^{13}\text{C}$ – $^1\text{H}$  decoupling (decoupling effect) using the radiofrequency field on the resonance frequency of protons [28]. Samples ( $\sim 100$  mg) were placed in a  $\text{ZrO}_2$  4.0-mm ceramic rotor. For  $^{13}\text{C}$  MAS NMR measurements, rotation at the magic angle at a frequency of 4700–5600(1) Hz was used, the scan number was 3800–6800, the duration of proton  $\pi/2$  pulses was 4.9–5.0  $\mu\text{s}$ , the  $^1\text{H}$ – $^{13}\text{C}$  contact time was 2.0–2.5 ms, and the interval between pulses was 3.0 s. Isotropic chemical shifts ( $^{13}\text{C}$   $\delta$ ) are given relatively to one of the components of crystalline adamantane used as an external standard [29] ( $\delta = 38.48$  ppm, relative to tetramethylsilane [30]).

**X-ray diffraction analysis** was carried out at 170(2) K from a prismatic single crystal of compound **I** on a BRUKER Kappa APEX II diffractometer ( $\text{MoK}_\alpha$  radiation,  $\lambda = 0.71073$  Å, graphite monochromator), the crystal–detector distance being 45 mm. An X-ray absorption correction was applied by the indices of crystal faces. The structure was determined by a direct method and refined by least squares (for  $F^2$ ) in the full-matrix anisotropic approximation for non-hydrogen atoms. The positions of hydrogen atoms were calculated geometrically and included into refinement in the riding model. Each atom in the centrosymmetric binuclear anion  $[\text{Au}_2\text{Cl}_8]^{2-}$  ( $\text{Au}(4)$ ,  $\text{Cl}(4)$ ,  $\text{Cl}(5)$ ,  $\text{Cl}(6)$ , and  $\text{Cl}(7)$ ) is statistically distributed between two positions *A* and *B* with site occupancies of 0.696(2) and 0.304(2), respectively.

Data collection and editing and the refinement of unit cell parameters were performed using the APEX2 [31] and SAINT [32] programs. Calculations on structure determination and refinement were performed using the SHELXTL/PC programs [33].

**Table 1.** Crystallographic data and the experimental and refinement parameters for structure **I**

Parameter	Value
Empirical formula	$C_{30}H_{48}N_6O_6S_{12}Cl_{12}Au_6$
FW	2580.66
Crystal system	Monoclinic
Space group	$C2/c$
$a, \text{\AA}$	24.8729(10)
$b, \text{\AA}$	9.5087(4)
$c, \text{\AA}$	27.4353(11)
$\beta, \text{deg}$	105.082(2)
$V, \text{\AA}^3$	6265.2(4)
$Z$	4
$\rho_{\text{calcd}}, \text{g/cm}^3$	2.736
$\mu, \text{mm}^{-1}$	14.953
$F(000)$	4752
Crystal size, mm	Prism (0.39 $\times$ 0.32 $\times$ 0.16)
Data collection range on $\theta, \text{deg}$	2.30–40.89
Ranges of $h, k$ , and $l$ indices	$-45 \leq h \leq 45$ , $-17 \leq k \leq 17$ , $-50 \leq l \leq 50$
Number of measured reflections	73800
Number of independent reflections ( $R_{\text{int}}$ )	20392 (0.0288)
Number of reflections with $I > 2\sigma(I)$	15452
Number of refined variables	374
Goodness-of-fit	1.022
$R$ factors for $F^2 > 2\sigma(F^2)$	$R_1 = 0.0291, wR_2 = 0.0595$
$R$ factors for all reflections	$R_1 = 0.0483, wR_2 = 0.0651$
Residual electron density (min/max), $e/\text{\AA}^3$	-2.191/2.745

The main crystallographic data and the results of structure **I** refinement are presented in Table 1. Selected bond lengths and angles are given in Table 2. The coordinates of atoms, bond lengths, and angles were deposited with the Cambridge Crystallographic Data Centre (no. 912945; deposit@ccdc.cam.ac.uk or <http://www.ccdc.cam.ac.uk>).

The thermal properties of compound **I** were studied by the STA method including the simultaneous detection of thermogravimetric (TG) and differential scanning calorimetric (DSC) curves. The study was carried out on an STA 449C Jupiter instrument (NETZSCH)

in corundum crucibles under a cap with a hole providing a vapor pressure of 1 atm upon the thermal decomposition of the sample. The heating rate was 5°C/min up to 1100°C in an argon atmosphere. The sample weight was 2.353–3.322 mg. The accuracy of temperature measurements was  $\pm 0.7^\circ\text{C}$ , and that of the weight change was  $\pm 1 \times 10^{-4}$  mg.

## RESULTS AND DISCUSSION

The data showing the dependence of the degree of sorption of gold(III) on the time of contact of sorbents **Ia** and **Ib** with solutions of  $\text{AuCl}_3$  in the static mode are presented in Table 3. Working solutions with two different concentrations (Table 3) each 10 mL in volume were used. According to the data in Table 3, a higher degree of sorption of gold(III) from solution is achieved when sorbent **Ia** is used. White precipitates of the used sorbents rearranged already during the first minutes of contact with the working solutions accompanied by the visualized enlargement of the particles, a change in the color to yellow-orange, and the gradual transition of the color to bright yellow. These changes indicate the formation of new compounds in the sorption systems studied. To reveal these new compounds, gold-saturated sorbents **Ia** and **Ib** were dissolved in acetone. Identical yellow transparent crystals of polynuclear complex **I**, whose crystal and supramolecular structures were determined by X-ray diffraction analysis, were obtained from solutions. The theoretical chemisorption capacity of cadmium and zinc morpholinedithiocarbamates with respect to gold(III) was estimated by the consideration of the reactions of synthesis of complex **I** as 901.7 and 1010.4 mg of  $\text{Au}^{3+}$  per 1 g of sorbents, respectively.

According to the  $^{13}\text{C}$  MAS NMR data, the polycrystalline samples preparatively isolated from the both chemisorption systems are spectrally identical. The  $^{13}\text{C}$  MAS NMR spectrum (Fig. 1) of compound **I** contains resonance signals assigned to the  $=\text{NC}(\text{S})\text{S}-$ ,  $-\text{OCH}_2-$ , and  $=\text{NCH}_2-$  groups (see section Synthesis). As compared to the initial cadmium and zinc complexes,  $\delta(^{13}\text{C})$  of the dithiocarbamate groups in compound **I** are characterized by substantially lower values. This can be due to the coordination of the Mfdtc ligands by gold (the electronic system of the latter is more efficiently involved in the additional shielding of the carbon nuclei of the  $=\text{NC}(\text{S})\text{S}-$  groups due to the heavy atom effect). The fragment-to-fragment mathematical simulation of the spectrum made it possible to refine the ratio of integral intensities of the  $^{13}\text{C}$  signals from three (1 : 1 : 1) structurally nonequivalent  $=\text{NC}(\text{S})\text{S}-$  groups and, correspondingly, six (1 : 2 : 3)  $-\text{OCH}_2-$  and (1 : 1 : 4)  $=\text{NCH}_2-$  groups. All this indicates a complicated structural organization of new compound **I** formed in the  $[\text{M}\{\text{S}_2\text{CN}(\text{CH}_2)_4\text{O}\}_2]_n - [\text{AuCl}_4]^-/2 \text{M HCl}$  ( $\text{M} = \text{Cd, Zn}$ ) systems. To check these conclusions, the molecular and supramolecular

**Table 2.** Selected bond lengths (*d*) and the bond ( $\omega$ ) and torsion ( $\phi$ ) angles in structure I

Complex cation A			
Bond	<i>d</i> , Å	Bond	<i>d</i> , Å
Au(1)–S(1)	2.3335(7)	S(4)–C(6)	1.723(3)
Au(1)–S(2)	2.3313(7)	N(1)–C(1)	1.298(4)
Au(1)–S(3)	2.3443(7)	N(1)–C(2)	1.471(4)
Au(1)–S(4)	2.3185(7)	N(1)–C(5)	1.469(4)
S(1)–C(1)	1.734(3)	N(2)–C(6)	1.310(4)
S(2)–C(1)	1.726(3)	N(2)–C(7)	1.477(4)
S(3)–C(6)	1.726(3)	N(2)–C(10)	1.477(4)
Angle	$\omega$ , deg	Angle	$\omega$ , deg
S(1)Au(1)S(2)	75.64(2)	S(2)C(1)N(1)	124.5(2)
S(1)Au(1)S(3)	105.98(2)	S(1)C(1)S(2)	111.48(15)
S(1)Au(1)S(4)	178.38(2)	S(3)C(6)N(2)	125.6(2)
S(2)Au(1)S(3)	177.87(3)	S(4)C(6)N(2)	122.4(2)
S(2)Au(1)S(4)	102.75(2)	S(3)C(6)S(4)	111.97(15)
S(3)Au(1)S(4)	75.63(2)	C(1)N(1)C(2)	123.6(2)
Au(1)S(1)C(1)	86.31(9)	C(1)N(1)C(5)	123.7(2)
Au(1)S(2)C(1)	86.57(9)	C(2)N(1)C(5)	112.7(2)
Au(1)S(3)C(6)	85.76(10)	C(6)N(2)C(7)	121.7(2)
Au(1)S(4)C(6)	86.64(9)	C(6)N(2)C(10)	124.1(2)
S(1)C(1)N(1)	124.0(2)	C(7)N(2)C(10)	114.1(2)
Angle	$\phi$ , deg	Angle	$\phi$ , deg
Au(1)S(1)S(2)C(1)	−179.8(2)	S(2)C(1)N(1)C(2)	179.8(2)
S(1)Au(1)C(1)S(2)	−179.8(2)	S(2)C(1)N(1)C(5)	−0.6(4)
Au(1)S(3)S(4)C(6)	179.0(2)	S(3)C(6)N(2)C(7)	177.4(2)
S(3)Au(1)C(6)S(4)	179.2(2)	S(3)C(6)N(2)C(10)	1.0(4)
S(1)C(1)N(1)C(2)	1.7(4)	S(4)C(6)N(2)C(7)	−2.6(4)
S(1)C(1)N(1)C(5)	−178.7(2)	S(4)C(6)N(2)C(10)	−179.1(2)
Complex cation B			
Bond	<i>d</i> , Å	Bond	<i>d</i> , Å
Au(2)–S(5)	2.3319(6)	S(6)–C(11)	1.731(3)
Au(2)–S(6)	2.3210(7)	N(3)–C(11)	1.298(3)
Au(2)…S(4)	3.6364(8)	N(3)–C(12)	1.464(4)
Au(2)…S(4) <sup>b</sup>	3.6364(8)	N(3)–C(15)	1.474(4)
S(5)–C(11)	1.729(3)		
Angle	$\omega$ , deg	Angle	$\omega$ , deg
S(5)Au(2)S(6)	75.52(2)	S(5)C(11)N(3)	125.1(2)
S(5)Au(2)S(6) <sup>b</sup>	104.48(2)	S(6)C(11)N(3)	124.1(2)
S(5)Au(2)S(5) <sup>b</sup>	180.00(3)	S(5)C(11)S(6)	110.85(14)
S(4)Au(2)S(4) <sup>b</sup>	180.00(3)	C(11)N(3)C(12)	122.9(2)
Au(2)S(5)C(11)	86.64(9)	C(11)N(3)C(15)	122.8(2)
Au(2)S(6)C(11)	86.94(9)		
Angle	$\phi$ , deg	Angle	$\phi$ , deg
Au(2)S(5)S(6)C(11)	177.6(2)	S(5)C(11)N(3)C(15)	176.8(2)
S(5)Au(2)C(11)S(6)	177.8(2)	S(6)C(11)N(3)C(12)	−178.8(3)
S(5)C(11)N(3)C(12)	0.5(4)	S(6)C(11)N(3)C(15)	−2.5(4)

**Table 2.** (Contd.)

Complex anion C			
Bond	<i>d</i> , Å	Angle	$\omega$ , deg
Au(3)–Cl(1)	2.2770(13)	Cl(1)Au(3)Cl(2)	90.09(3)
Au(3)–Cl(2)	2.2792(9)	Cl(1)Au(3)Cl(3)	180.0
Au(3)–Cl(2) <sup>c</sup>	2.2792(9)	Cl(2)Au(3)Cl(2) <sup>c</sup>	179.81(6)
Au(3)–Cl(3)	2.2787(14)	Cl(2)Au(3)Cl(3)	89.91(2)

Complex anion D**			
Bond	<i>d</i> , Å	Bond	<i>d</i> , Å
Au(4A)–Cl(4A)	2.298(3)	Au(4B)–Cl(4B)	2.236(6)
Au(4A)–Cl(5A)	2.2553(14)	Au(4B)–Cl(5B)	2.252(4)
Au(4A)–Cl(6A)	2.2910(12)	Au(4B)–Cl(6B)	2.267(5)
Au(4A)–Cl(7A)	2.2660(17)	Au(4B)–Cl(7B)	2.314(4)
Au(4A)…Cl(5A) <sup>f</sup>	3.486(2)	Au(4B)…Cl(6B) <sup>f</sup>	3.985(5)
Au(4A) <sup>f</sup> …Cl(5A)	3.486(2)	Au(4B) <sup>f</sup> …Cl(6B)	3.985(5)

Angle	$\omega$ , deg	Angle	$\omega$ , deg
Cl(4A)Au(4A)Cl(5A)	90.03(9)	Cl(4B)Au(4B)Cl(5B)	92.1(3)
Cl(4A)Au(4A)Cl(6A)	89.70(9)	Cl(4B)Au(4B)Cl(6B)	87.7(3)
Cl(4A)Au(4A)Cl(7A)	176.79(10)	Cl(4B)Au(4B)Cl(7B)	177.6(3)
Cl(5A)Au(4A)Cl(6A)	177.82(7)	Cl(5B)Au(4B)Cl(6B)	179.73(13)
Cl(5A)Au(4A)Cl(7A)	89.26(6)	Cl(5B)Au(4B)Cl(7B)	90.2(2)
Cl(6A)Au(4A)Cl(7A)	91.13(6)	Cl(6B)Au(4B)Cl(7B)	89.9(2)

\* Symmetry transforms: <sup>b</sup>  $-x + 2, -y, -z$ ; <sup>c</sup>  $-x + 2, y, -z + 1/2$ ; <sup>f</sup>  $-x + 3/2, -y + 1/2, -z$ .

\*\* The occupancies of positions *A* and *B* are 0.696(2) and 0.304(2), respectively.

**Table 3.** Kinetics of gold(III) binding by sorbents **Ia** and **Ib**

Concentration of Au <sup>3+</sup> , mg/mL (solution volume 10 mL)	Degree of sorption (%) for contact duration, min					
	1	10	20	30	60	90
8.94 ( <b>Ia</b> )	84.45	93.85	94.91	95.21	95.57	96.06
10.05 ( <b>Ib</b> )	78.21	81.65	82.99	83.72	86.75	88.40

structures of the synthesized complex were solved by X-ray diffraction analysis.

The unit cell of ionic complex **I** includes four formula units  $[\text{Au}\{\text{S}_2\text{CN}(\text{CH}_2)_4\text{O}\}_2]_3[\text{Au}_2\text{Cl}_8][\text{AuCl}_4]$  (Fig. 2). Of twelve complex cations

$[\text{Au}\{\text{S}_2\text{CN}(\text{CH}_2)_4\text{O}\}_2]^+$ , eight noncentrosymmetric cations (A) with the Au(1) atom are structurally non-equivalent to four other cations: centrosymmetric cations (B) with the Au(2) atom (Table 2). At the supramolecular level, the cations discussed are self-organized into linear (angle Au(1)…Au(2)…Au(1)

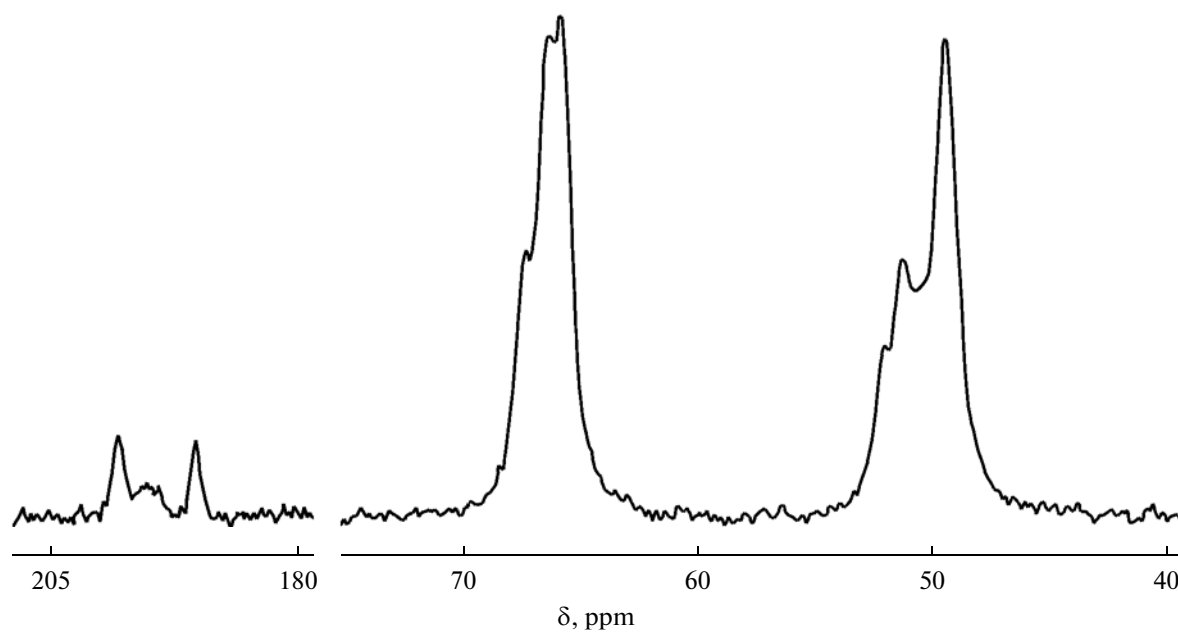


Fig. 1.  $^{13}\text{C}$  MAS NMR spectrum of complex I (scan number/rotation frequency 3800/5600).

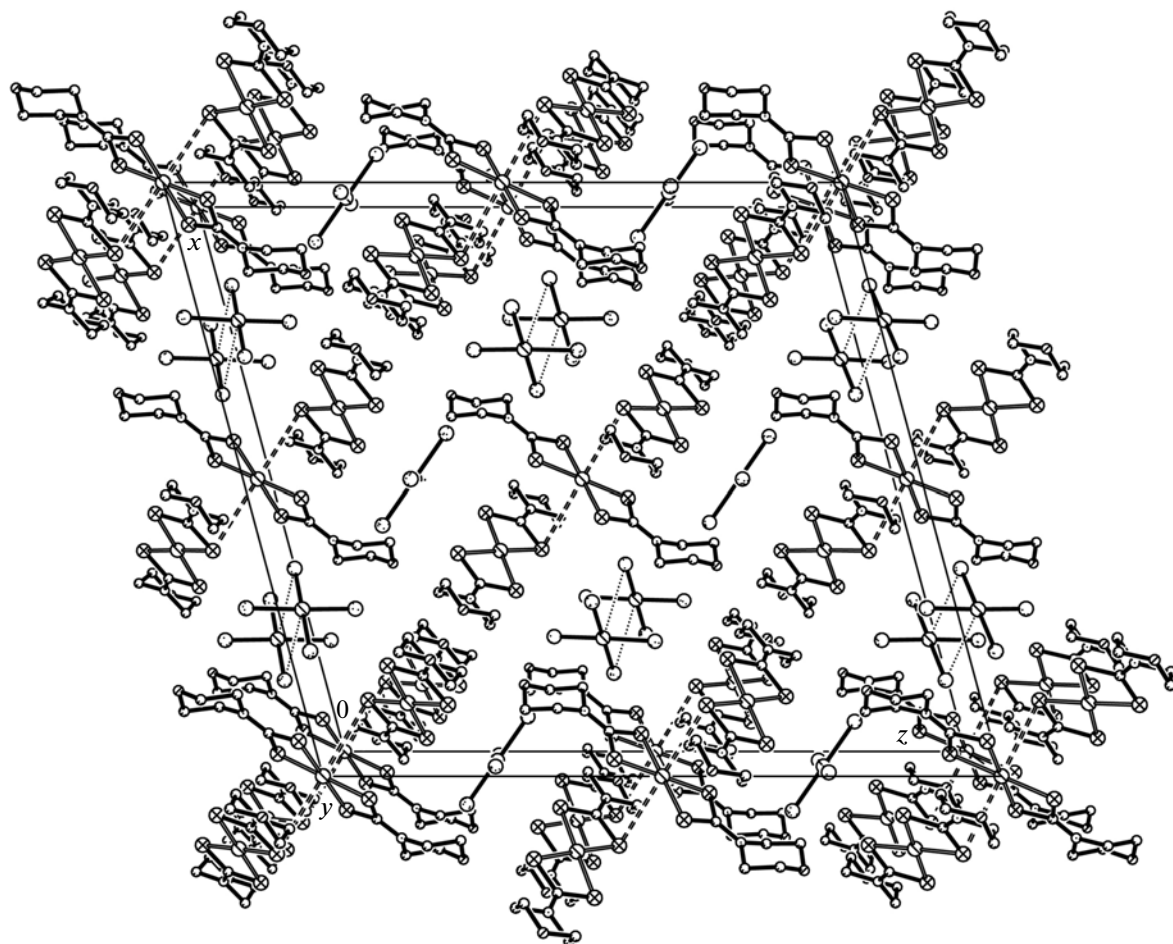
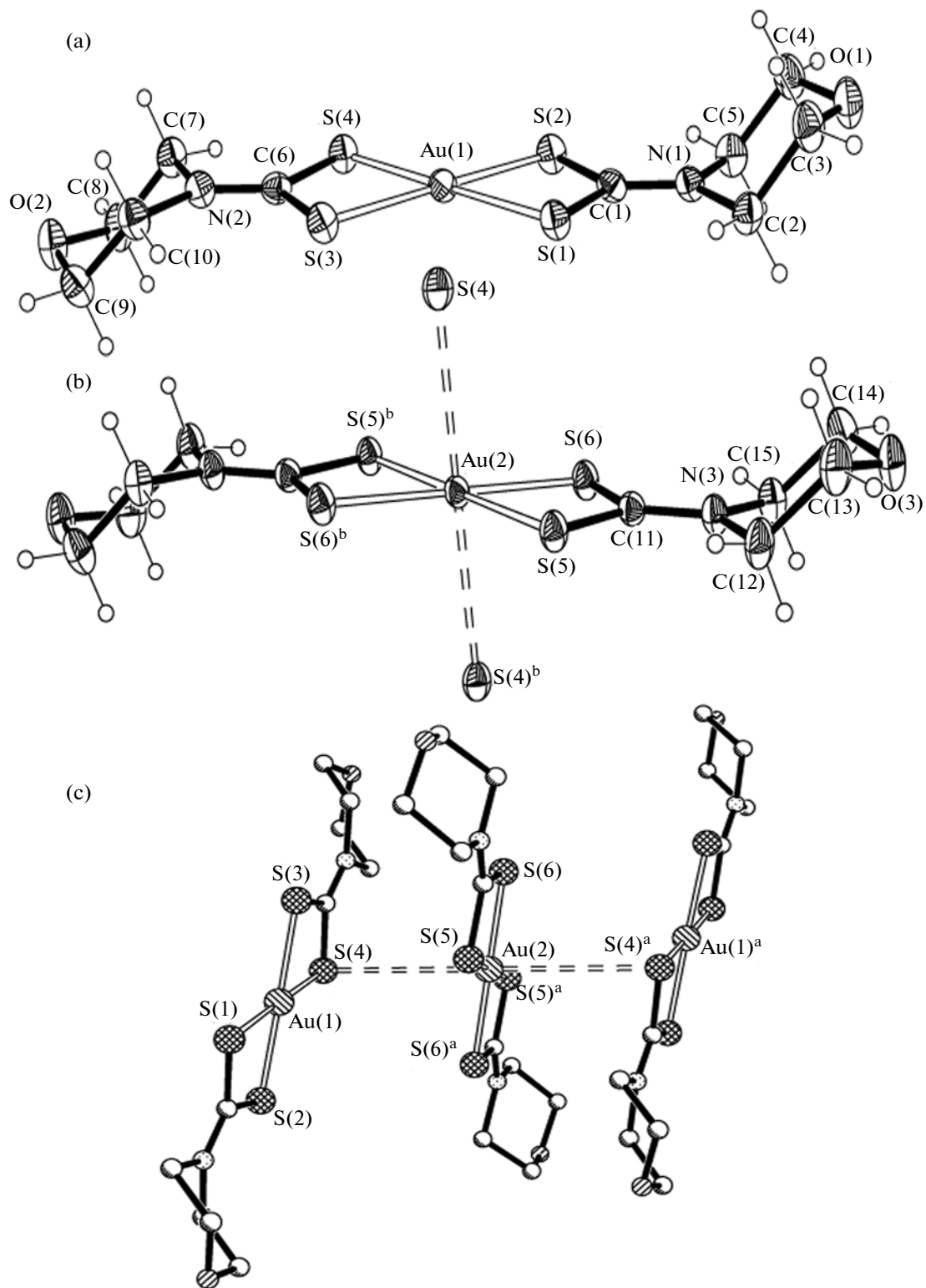


Fig. 2. Unit cell of compound I (projection onto the  $xz$  plane).



**Fig. 3.** Structures of the isomeric complex cations  $[\text{Au}\{\text{S}_2\text{CN}(\text{CH}_2)_4\text{O}\}_2]^+$ : conformers (a) A and (b) B and (c) the trinuclear cation  $[\text{Au}_3\{\text{S}_2\text{CN}(\text{CH}_2)_4\text{O}\}_6]^{3+}$ . The  $\text{Au}\cdots\text{S}$  secondary bonds are shown by dashed lines, displacement ellipsoids are at the 50% probability level.

180°) trinuclear structural fragments  $[\text{Au}_3\{\text{S}_2\text{CN}(\text{CH}_2)_4\text{O}\}_6]^{3+}$  of the  $[\text{A} \cdots \text{B} \cdots \text{A}]$  type (Fig. 3) due to secondary  $\text{Au} \cdots \text{S}$  bonds of 3.6364 Å, which somewhat exceeds the sum of van der Waals radii of gold and sulfur atoms (3.46 Å) [35–37]. The charges of trinuclear cations  $[\text{Au}_3\{\text{S}_2\text{CN}(\text{CH}_2)_4\text{O}\}_6]^{3+}$  compensate complex anions  $[\text{AuCl}_4]^-$  (C) and  $[\text{Au}_2\text{Cl}_8]^{2-}$  (D) alternating in the crystal structure at the right and left from the cations (Fig. 2). Mononuclear anions C are characterized by the square structure ( $dsp^2$ -hybrid state of gold; the  $\text{Au}(3)$ ,  $\text{Cl}(1)$ , and  $\text{Cl}(3)$  atoms lie on the double rotation axis). Centrosymmetric binuclear anions D are formed due to joining the  $[\text{AuCl}_4]^-$  anions by two secondary  $\text{Au} \cdots \text{Cl}$  bonds: 3.486 Å  $\text{Au}(4A) \cdots \text{Cl}(5A)^f$  or 3.985 Å  $(\text{Au}(4B) \cdots \text{Cl}(6B)^f)$  (Fig. 4). The length of the latter noticeably exceeds the sum of van der Waals radii of gold and chlorine atoms (3.41 Å) [35–37]. In addition, the discussed structural situation is complicated by the fact that in the  $[\text{Au}_2\text{Cl}_8]^{2-}$  anion each atom ( $\text{Au}(4)$ ,  $\text{Cl}(4)$ ,  $\text{Cl}(5)$ ,  $\text{Cl}(6)$ , and  $\text{Cl}(7)$ ) is statistically distributed between two positions A (Fig. 4a) and B (Fig. 4b) with different site occupancies: 0.696(2) and 0.304(2), respectively.

Let us consider the structure of the complex cations  $[\text{Au}\{\text{S}_2\text{CN}(\text{CH}_2)_4\text{O}\}_2]^+$  in more detail. In each cation (centrosymmetric and noncentrosymmetric), the internal coordination sphere of each gold atom includes two  $\text{Mfdtc}$  ligands. In noncentrosymmetric cation A, the coordination of one ligand is close to  $S,S'$ -isobidentate ( $\text{Au} \cdots \text{S}$  2.3313 and 2.3335 Å), while the second ligand is anisobidentately coordinated ( $\text{Au} \cdots \text{S}$  2.3185 and 2.3443 Å). In centrosymmetric cation B, the ligands also exhibit the anisobidentate binding mode ( $\text{Au} \cdots \text{S}$  2.3185 and 2.3319 Å). In spite of the same structural type of nonequivalent complex cations A and B, the lengths of the corresponding bonds ( $\text{Au} \cdots \text{S}$ ,  $\text{C} \cdots \text{S}$ ,  $\text{N} \cdots \text{C}(\text{S})\text{S}$ ), and the values of bond ( $\text{SAuS}$ ,  $\text{SCS}$ ) and torsion angles ( $\text{SCNC}$ ) exhibit reliable distinctions, which makes it possible to classify them as conformational isomers. We have earlier identified conformers of the dithiocarbamate complexes for the whole series of other metals [38–43].

According to the results of the described coordination mode, the metal atom is surrounded by four sulfur atoms. The arrangement of the atoms in the  $[\text{AuS}_4]$  chromophores is close to coplanar, which indicates the low-spin intraorbital  $dsp^2$ -hybrid state of gold(III). In the rectangular chromophores, the short side is determined by intraligand  $\text{S} \cdots \text{S}$  distances of 2.849–2.861 Å and the long side is determined by interligand  $\text{S} \cdots \text{S}$  distances of 3.633–3.735 Å. The latter values are close to the doubled van der Waals radius of the sulfur atom

<sup>1</sup> The concept of secondary bonds has first been proposed [34] for the explanation of interactions at distances comparable with the sums of van der Waals radii of the corresponding pairs of atoms.

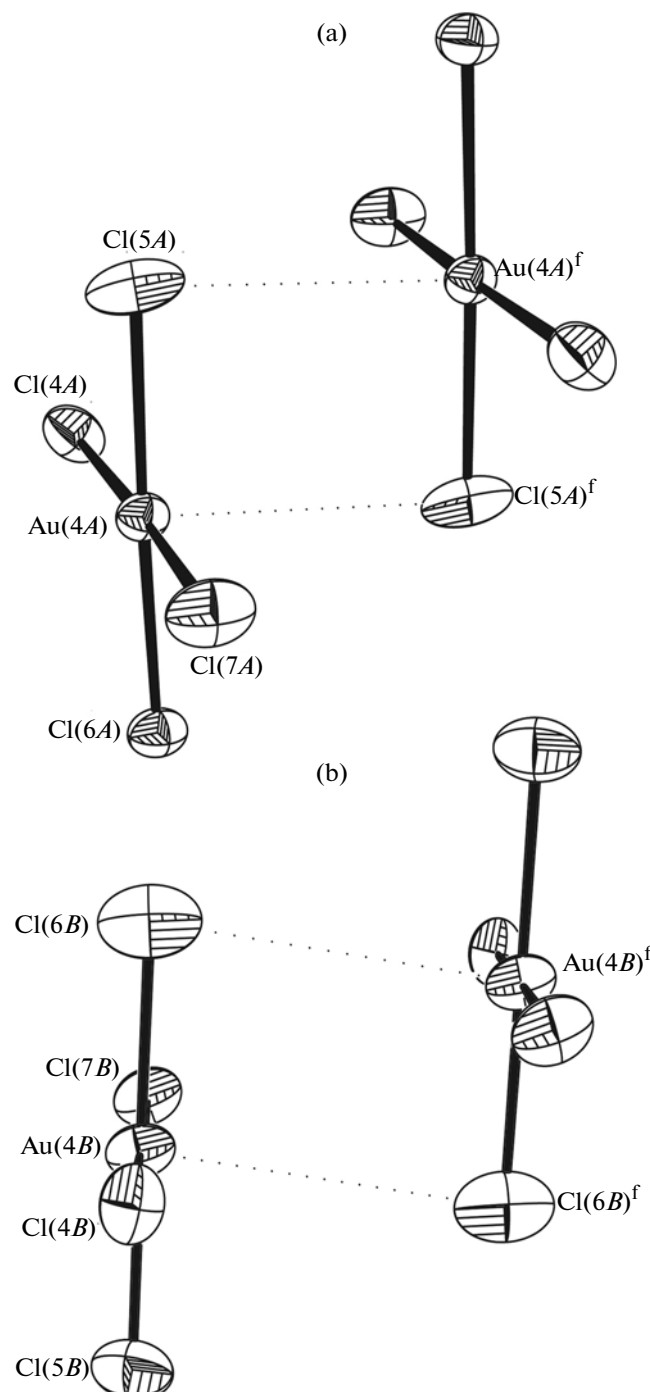


Fig. 4. Structure of the binuclear complex anion  $[\text{Au}_2\text{Cl}_8]^{2-}$  with all atoms in positions (a) A and (b) B. The  $\text{Au} \cdots \text{Cl}$  secondary bonds are shown by dashed lines, displacement ellipsoids are at the 50% probability level.

(3.60 Å) [35–37], whereas the former are substantially shorter. In cation B, the  $\text{Au}(2)$  atom in the axial position additionally forms two secondary  $\text{Au} \cdots \text{S}$  bonds with adjacent cations A and, on the whole, is situated at the center of a strongly extended octahedron of six sulfur atoms (Fig. 3c).

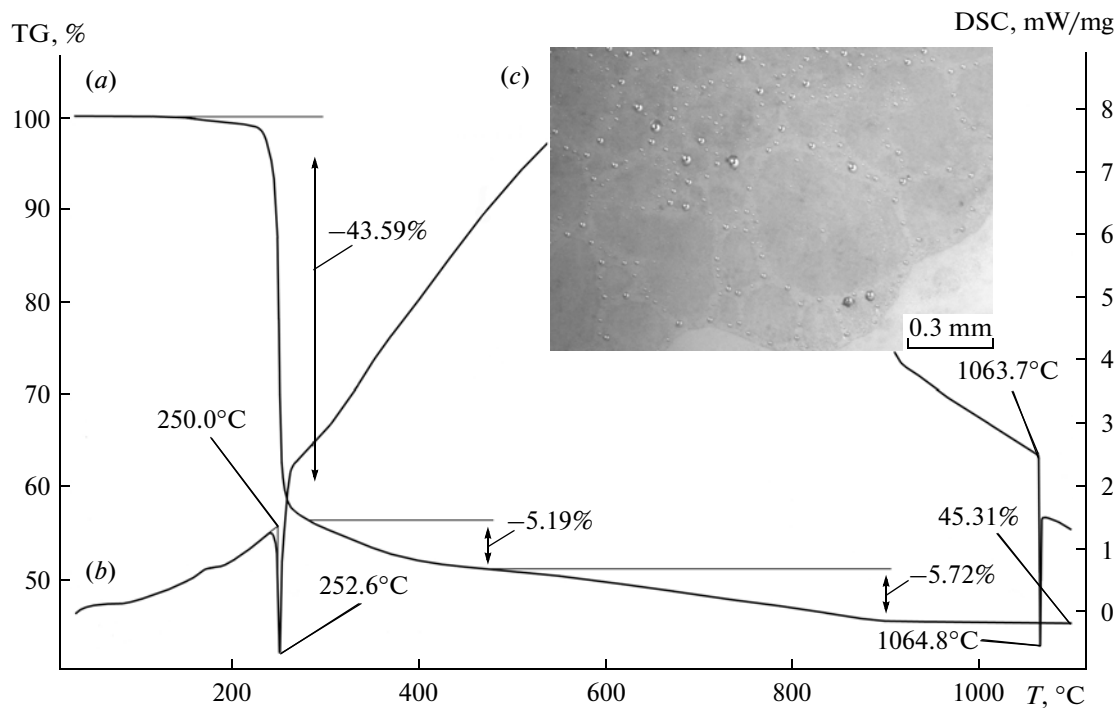


Fig. 5. (a) TG and (b) DSC curves for complex I. (c) Enlarged fragment of the crucible bottom after passing m.p.

In each cation A and B, the bidentate coordination of the Mfdtc ligands results in the formation of two four-membered almost planar metallocycles  $\text{AuS}_2\text{C}$  (the values of  $\text{AuSSC}$  and  $\text{SAuCS}$  torsion angles do not strongly deviate from  $180^\circ$ ). The discussed cycles are bound by the common gold atom to form the bicyclic structural fragment  $\text{CS}_2\text{AuS}_2\text{C}$ . The distances between the opposite gold and carbon atoms in the cycles ( $2.807$ – $2.820$  Å) are substantially shorter than the sum of their van der Waals radii ( $3.36$  Å) [40–42] and indicate the direct interaction between the discussed atoms directly through the space of small-sized metallocycles (*trans*-annular interaction).

The  $\text{C}_2\text{NC}(\text{S})\text{S}$  groups in the Mfdtc ligands are nearly planar: the  $\text{SCNC}$  torsion angles are close to  $180^\circ$  or  $0^\circ$  (Table 2). The second feature of dithiocarbamate groups is a higher strength of the  $\text{N}-\text{C}(\text{S})\text{S}$  bonds ( $1.298$  and  $1.310$  Å for conformer A,  $1.298$  Å for conformer B) as compared to the  $\text{N}-\text{CH}_2$  bonds (Table 2). These circumstances are a direct indication to the mesomeric effect manifested in the Dtc groups. In all the three Mfdtc ligands, the morpholine heterocycles take a chair conformation: the angles inside the cycles are  $108.2^\circ$ – $112.3^\circ$  (admixing of the  $sp^2$ -hybrid state of the nitrogen atoms results in an increase in the CNC angles to  $112.7^\circ$ – $114.1^\circ$ ), the  $\text{C}-\text{O}$  bond lengths are  $1.413$ – $1.425$  Å, and  $\text{C}-\text{N}$  are  $1.464$ – $1.477$  Å. In both cations, the heterocycles relatively to the  $[\text{AuS}_4]$  chromophore plane are oriented in opposite directions (Fig. 3).

The regeneration conditions of chemisorbed gold were revealed by the STA study of the thermal properties of compound I. The TG curve (Fig. 5a) shows the thermal stability of complex I below  $145^\circ\text{C}$  and includes three stages of weight loss: first ( $145$ – $283^\circ\text{C}$ ), second ( $283$ – $470^\circ\text{C}$ ), and third ( $470$ – $905^\circ\text{C}$ ). The steep-grade region of the TG curve at the first stage shows the main weight loss equal to  $43.59\%$ , which indicates that the thermolysis of compound I occurs simultaneously at the cation and anions with the partial reduction to metallic gold. For the process discussed, the corresponding region of the DSC curve (Fig. 5b) detects an intense endotherm with an extreme at  $252.6^\circ\text{C}$ . The independent determination of m.p. in a glass capillary for complex I made it possible to establish melting with decomposition (accompanied by vigorous gas evolution) at  $250^\circ\text{C}$ , which exactly coincides with the extrapolated m.p. ( $250.0^\circ\text{C}$ ) obtained from the calculation of the DSC curve. The most probable intermediates of gold reduction are  $\text{Au}_2\text{S}$  (for the cationic part) and  $\text{AuCl}$  (thermolysis of anions). The temperature of decomposition of  $\text{Au}_2\text{S}$   $240^\circ\text{C}$  [44]) falls onto the steep-grade region of the TG curve and, hence, the decomposition of  $\text{Au}_2\text{S}$  is not detected by a particular step. The decomposition temperature of  $\text{AuCl}$  is somewhat higher ( $289^\circ\text{C}$  [44]). Therefore, the second stage of thermolysis ( $283$ – $470^\circ\text{C}$ ) presented by a weakly pronounced step with a weight loss of  $5.19\%$  can mainly be assigned to the decomposition of  $\text{AuCl}$  (calcd.  $4.12\%$ ) against the background of desorption of the thermolysis prod-

ucts formed at the first stage. The last stage (with 470°C to the stabilization of the residual weight at 905.0°C) is due to the smooth desorption of the thermolysis products of compound **I** (5.72%). The final thermolysis product is reduced metallic gold: the DSC curve detects the endotherm of its melting (the extrapolated m.p. is 1063.7°C). At 1100°C a residual weight of 45.31% does not strongly deviate from a theoretical value of 45.79%. Finely dispersed gold in the form of finest red-pink sputtering and gold balls 0.001–0.05 mm in diameter were observed on the bottom of the crucible (Fig. 5c).

### ACKNOWLEDGMENTS

The authors are grateful to Prof. O.N. Antzutkin (Luleå University of Technology, Sweden) for the kindly presented possibility of recording  $^{13}\text{C}$  MAS NMR spectra.

This work was supported by the Presidium of the Russian Academy of Sciences (program for basic research “Development of Methods for Synthesis of Chemical Substances and Production of New Materials”) and the Presidium of the Far East Branch of the Russian Academy of Sciences (projects nos. 12-I-P8-01 and 12-III-A-04-040).

### REFERENCES

- Ajibade, P.A., Onwudiwe, D.C., and Moloto, M.J., *Polyhedron*, 2011, vol. 30, no. 2, p. 246.
- Srinivasan, N., Thirumaran, S., and Ciattini, S., *J. Mol. Struct.*, 2012, vol. 1026, p. 102.
- Srinivasan, N. and Thirumaran, S., *Superlatt. Microstruct.*, 2012, vol. 51, no. 6, p. 912.
- Ajibade, P.A. and Onwudiwe, D.C., *J. Mol. Struct.*, 2013, vol. 1034, p. 249.
- Rotaru, A., Mietlarek-Kropidlowska, A., Constantinescu, C., et al., *Appl. Surf. Sci.*, 2009, vol. 255, no. 15, p. 6786.
- Prakasam, B.A., Ramalingam, K., Bocelli, G., and Cantoni, A., *Polyhedron*, 2007, vol. 26, no. 15, p. 4489.
- Decken, A., Eisnor, C.R., Gossage, R.A., and Jackson, S.M., *Inorg. Chim. Acta*, 2006, vol. 359, no. 6, p. 1743.
- Decken, A., Gossage, R.A., Chan, M.Y., et al., *Appl. Organomet. Chem.*, 2004, vol. 18, no. 2, p. 101.
- Shahid, M., Ruffer, T., Lang, H., et al., *J. Coord. Chem.*, 2009, vol. 62, no. 3, p. 440.
- Saravanan, M., Ramalingam, K., Bocelli, G., and Olla, R., *Appl. Organomet. Chem.*, 2004, vol. 18, no. 2, p. 103.
- Loseva, O.V., Ivanov, A.V., Gerasimenko, A.V., et al., *Russ. J. Coord. Chem.*, 2010, vol. 36, no. 1, p. 1.
- Ivanov, A.V., Zinkin, S.A., Gerasimenko, A.V., and Sergienko, V.I., *Russ. J. Coord. Chem.*, 2011, vol. 37, no. 6, p. 452.
- Loseva, O.V., Rodina, T.A., Ivanov, A.V., et al., *Russ. J. Coord. Chem.*, 2011, vol. 37, no. 12, p. 897.
- Rodina, T.A., Ivanov, A.V., Gerasimenko, A.V., et al., *Polyhedron*, 2012, vol. 40, no. 1, p. 53.
- Rodina, T.A., Ivanov, A.V., Loseva, O.V., et al., *Russ. J. Inorg. Chem.*, 2013, vol. 58, no. 3, p. 338.
- Rodina, T.A., Loseva, O.V., Gerasimenko, A.V., and Ivanov, A.V., *Russ. J. Inorg. Chem.*, 2013, vol. 58, no. 9, in press.
- Ronconi, L., Giovagnini, L., Marzano, C., et al., *Inorg. Chem.*, 2005, vol. 44, no. 6, p. 1867.
- Mansour, M.A., Connick, W.B., Lachicotte, R.J., et al., *J. Am. Chem. Soc.*, 1998, vol. 120, no. 6, p. 1329.
- Van Zyl, W.E., Lopez-de-Luzuriaga, J.M., Mohamed, A.A., et al., *Inorg. Chem.*, 2002, vol. 41, no. 17, p. 4579.
- Lee, Y.-A., McGarrah, J.E., Lachicotte, R.J., and Eisenberg, R., *J. Am. Chem. Soc.*, 2002, vol. 124, no. 36, p. 10662.
- Han, S., Jung, O.-S., and Lee, Y.-A., *Transition Met. Chem.*, 2011, vol. 36, no. 7, p. 691.
- Byr'ko, V.M., *Ditiokarbamaty* (Dithiocarbamates), Moscow: Nauka, 1984.
- Garcia-Fontan, S., Rodriguez-Seoane, P., Casas, J.S., et al., *Inorg. Chim. Acta*, 1993, vol. 211, no. 2, p. 211.
- Ivanov, A.V., Konzelko, A.A., Gerasimenko, A.V., et al., *Russ. J. Inorg. Chem.*, 2005, vol. 50, no. 11, p. 1710.
- Ivanov, A.V., Ivakhnenko, E.V., Gerasimenko, A.V., and Forsling, W., *Russ. J. Inorg. Chem.*, 2003, vol. 48, no. 1, p. 45.
- Hexem, J.G., Frey, M.H., and Opella, S.J., *J. Chem. Phys.*, 1982, vol. 77, no. 7, p. 3847.
- Harris, R.K., Jonsen, P., and Packer, K.J., *Magn. Reson. Chem.*, 1985, vol. 23, no. 7, p. 565.
- Pines, A., Gibby, M.G., and Waugh, J.S., *J. Chem. Phys.*, 1972, vol. 56, no. 4, p. 1776.
- Earl, W.L., VanderHart, D.L., *J. Magn. Reson.*, 1982, vol. 48, no. 1, p. 35.
- Morcombe, C.R. and Zilm, K.W., *J. Magn. Reson.*, 2003, vol. 162, no. 2, p. 479.
- APEX2. Madison (WI, USA): Bruker AXS, 2010.
- SAINT. Madison (WI, USA): Bruker AXS, 2010.
- Sheldrick, G.M., *Acta Crystallogr., Sect. A: Found. Crystallogr.*, 2008, vol. 64, p. 112.
- Alcock, N.W., *Adv. Inorg. Chem. Radiochem.*, 1972, vol. 15, no. 1, p. 1.
- Pauling, L., *The Nature of the Chemical Bond and the Structure of Molecules and Crystals*, London: Cornell Univ., 1960.
- Bondi, A., *J. Phys. Chem.*, 1964, vol. 68, no. 3, p. 441.
- Bondi, A., *J. Phys. Chem.*, 1966, vol. 70, no. 9, p. 3006.
- Ivanov, A.V., Mitrofanova, V.I., Kritikos, M., and Antzutkin, O.N., *Polyhedron*, 1999, vol. 18, no. 15, p. 2069.
- Ivanov, A.V., Kritikos, M., Antzutkin, O.N., and Forsling, W., *Inorg. Chim. Acta*, 2001, vol. 321, nos. 1–2, p. 63.
- Ivanov, A.V., Pakusina, A.P., Ivanov, M.A., et al., *Dokl. Phys. Chem.*, 2005, vol. 401, no. 2, p. 44.
- Ivanov, A.V., Zaeva, A.S., Gerasimenko, A.V., and Forsling, W., *Dokl. Phys. Chem.*, 2005, vol. 404, no. 2, p. 205.
- Ivanov, A.V. and Antzutkin, O.N., *Topics Curr. Chem.*, 2005, vol. 246, p. 271.
- Ivanov, A.V., Gerasimenko, A.V., Konzelko, A.A., et al., *Inorg. Chim. Acta*, 2006, vol. 359, no. 12, p. 3855.
- Lidin, R.A., Andreeva, L.L., and Molochko, V.A., *Spravochnik po neorganicheskoi khimii* (Reference Book in Inorganic Chemistry), Moscow: Khimiya, 1987.

Translated by E. Yablonskaya